Cyclotron Resonance Maser Experiment in a Nondispersive Waveguide

Eli Jerby, Avi Shahadi, Rami Drori, Michael Korol, Moshe Einat, Marat Sheinin, Vladimir Dikhtiar, Vladimir Grinberg, Moshe Bensal, Tal Harhel, Yitzchak Baron, Amnon Fruchtman, *Member, IEEE*, Victor L. Granatstein, *Fellow, IEEE*, and George Bekefi

***Abstract*—A cyclotron–resonance maser (CRM) oscillator experiment in which a spiraling electron beam interacts with a transverse electromagnetic wave in a nondispersive waveguide is presented. The experiment employs a low-energy (<5 keV) low-current (<1 A) electron beam in a two-wire (Lecher type) waveguide. The microwave output frequency is tuned in this experiment by the axial magnetic field in the range 3.5–6.0 GHz. A second harmonic emission is observed at ~7 GHz. CRM theory shows that in a free-space TEM-mode interaction, the gain might be canceled due to the equal and opposite effects of the axial (Weibel) and the azimuthal bunching mechanisms. This balance is violated in the large transverse velocity regime ($V_\perp \gg V_z$) in which our experiment operates. The tunability measurements of the CRM oscillator experiment in the nondispersive waveguide are discussed in view of the CRM theory.**

I. Introduction

THE CYCLOTRON resonance maser (CRM) is well known as a high-power source of millimeter waves [1]. Early studies of the cyclotron resonance interaction were conducted in the late 1950's [2]–[4]. These studies were followed by various related experiments [5]–[10], including a demonstration of a CRM oscillator [7].

Relativistic electron beams were used in CRM experiments [11] in order to obtain high-power coherent millimeter waves. The gyrotron [12]–[16] was developed as a practical source for millimeter and submillimeter waves based on the cyclotron resonance interaction. Superconducting magnets are used in some gyrotron devices in order to increase the resonance frequency. The practical limit of the magnetic field strength motivates an intensive study of high-harmonic operation of cyclotron resonance masers [13], [17]–[20]. Another approach to increase the radiation frequency is by using the Doppler upshift in a cyclotron autoresonance maser (CARM) scheme [15], [21]–[23]. Recent theoretical studies on CRM and CARM interactions include nonlinear and self-consistent analysis, electron space charge effects, nonuniform magnetic fields, gyro-harmonic operation, and stability analysis [15], [24]–[29]. A gyrophase coherent electron beam has been proposed in order to increase the radiation gain [30].

The main interest of CRM studies has been *fast-wave* devices operating with TE and TM waveguide modes. Slow-wave cyclotron masers [31]–[38] have been investigated in various dielectric waveguides in order to increase the interaction bandwidth and to reduce the electron beam energy. The dominant mechanism of the slow-wave cyclotron maser is the axial bunching effect, known as the Weibel interaction. This effect opposes the azimuthal bunching effect which dominates in the fast-wave CRM interaction [39]. The periodic-waveguide cyclotron maser [40]–[43] is a device which can operate in both fast- and slow-wave modes. It has been demonstrated recently in amplifier [40] and oscillator [41], [42] experiments. A theoretical analysis of the periodic-waveguide cyclotron maser shows that it may operate in a fast-wave mode without an initial electron transverse velocity component [43].

Studies of CRM interactions with TEM waves were conducted early in the 1970's. In the low-gain regime, the TEM-wave interaction is expected to be weaker than with other modes [44], [45]. A CRM oscillator experiment operating in a Fabry–Perot cavity is described in [46]. It defines the condition for a CRM amplification in free-space as $V_\perp^2 > 2V_z c$, where $V_\perp$ and V_z are the electron perpendicular and axial velocity components. Other CRM experiments in Fabry–Perot resonators are reported in [47] and [48]. Theoretical studies of CRM interactions with TEM waves are devoted mainly to free-space propagation and to open resonators [49]–[54].

In this paper we describe a low-voltage table-top CRM oscillator in a nondispersive parallel-line waveguide which supports TEM waves. (To our best knowledge, this is the first CRM experiment reported in this scheme.) Radiation is observed in this experiment in a wide range of frequencies. The instability occurs whenever the electron beam acquires a large transverse velocity by a magnetic kicker at the entrance to the interaction region (note that the CRM theory does not predict gain in free-space TEM modes, except for the $V_\perp \gg V_z$ limit). A considerable emission at the second harmonic is observed as well. Theoretical aspects of the TEM-

Manuscript received August 7, 1995; revised February 23, 1996. This work was supported by the Israeli Ministry of Energy and the Belfer Foundation for Energy Research, the Israeli Ministry of Science, the Israeli Academy of Science, and the Avraham Schaterman Foundation.

E. Jerby, A. Shahadi, R. Drori, M. Korol, M. Einat, M. Sheinin, V. Dikhtiar, V. Grinberg, and M. Bensal are with the Faculty of Engineering, Tel Aviv University, Ramat Aviv 69978 Israel (e-mail: jerby@taunivm.tau.ac.il).

T. Harhel and Y. Baron are with the Technical College, Tel Aviv University, Ramat Aviv 69978 Israel.

A. Fruchtman is with the Center for Technological Education, Holon, Israel.

V. L. Granatstein is with the University of Maryland, College Park, MD 20742 USA.

G. Bekefi, deceased, was with the Department of Physics and Research Laboratory of Electronics, Massachusetts Institute of Technology, Cambridge, MA 02139 USA.

Publisher Item Identifier S 0093-3813(96)05188-0.

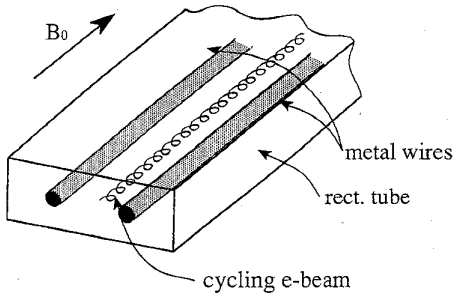

Fig. 1. Schematic of the TEM-mode cyclotron maser device.

mode cyclotron interaction are discussed in Section II. The experiment and its results are presented in Sections III and IV, respectively.

II. Theoretical Background

The cyclotron device used in our experiment is shown in Fig. 1 [55]. The metallic waveguide consists of a rectangular tube along which two parallel wires support odd and even TEM modes at frequencies below the empty waveguide cutoff. The feedback for oscillation buildup is provided by two metallic mirrors at both ends of the waveguide. A low-energy electron beam is orbiting in an externally applied axial magnetic field. The orbiting motion of the electrons couples them synchronously to the electromagnetic wave in the nondispersive waveguide.

The tuning relation of the cyclotron interaction is given in general by

$$\omega = n\omega_c \pm V_z k_z \tag{1}$$

where $\omega = kc$ is the electromagnetic (EM) wave angular frequency, k_z is the axial wavenumber, and n is the harmonic order. The $\pm$ signs correspond to interactions with forward and backward waves, as shown in the tuning diagram in Fig. 2. The angular cyclotron frequency is

$$\omega_c = \frac{e}{\gamma m} B_0 \tag{2}$$

where e, m, and γ are the electron charge, mass, and relativistic factor, respectively, and B_0 is the axial magnetic field.

The cyclotron interaction is described in the linear regime by a fourth-order Pierce-type dispersion equation [39], [43]. The transfer ratio of the electromagnetic wave at the fundamental harmonic ($n = 1$) along the interaction region is given in the Laplace complex-plane by

$$\tilde{T}(s,\omega) = \frac{(s - jk_z)[j(\omega - \omega_c) + V_z s]^2}{(s^2 + k_z^2)[j(\omega - \omega_c) + V_z s]^2 - Q_c(s,\omega)} \tag{3}$$

where the s variable is defined as a complex wavenumber in accordance with the known Laplace transform, $\tilde{T}(s) = \int_0^\infty T(z)e^{-sz}\,dz$. The coupling term between the EM wave

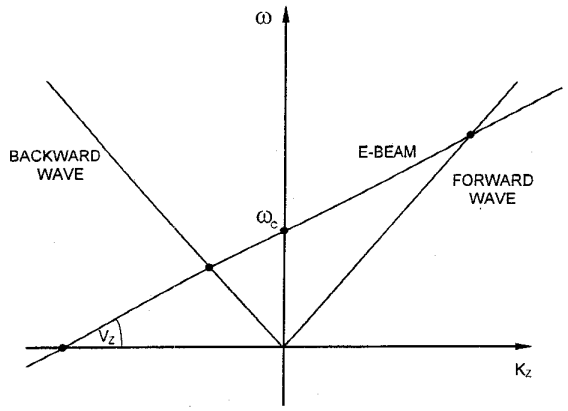

Fig. 2. The tuning diagram of the cyclotron interaction with a TEM wave.

and the cycling electron beam is

$$Q_c(s,\omega) = \frac{\omega_{pr}^2}{2c^2}\left\{(j\omega + V_z s)[j(\omega - \omega_c) + sV_z] + \frac{V_\perp^2}{2}(s^2 + k^2)\right\}. \tag{4}$$

The effective electron plasma frequency is $\omega_{pr} = (e^2 n_0 F_f/\epsilon_0 \gamma m)^{1/2}$, where ϵ_0 is the vacuum dielectric permittivity, n_0 is the electron beam density, and F_f is the effective filling-factor of the e beam in the interaction cross section.

The coupling term $Q_c(s,\omega)$ incorporates four different effects, each dominates in a different parameter regime as described in [39] and [43]. For a zero initial transverse electron velocity component ($V_\perp = 0$), the term $(j\omega + V_z s)$ in (4) represents the cyclotron absorption effect for $\omega > |V_z s|$ (as in our experiment). The opposite may occur in dielectric-loaded cyclotron masers [31]–[38], or periodic-waveguide cyclotron masers [40]–[43], in which the phase velocity of the EM wave might be considerably slow. Thus, for $\omega < |V_z s|$ and $\omega_c < 0$, a net amplification may be obtained without an initial rotation of the e beam (i.e., $V_\perp = 0$). This mechanism is associated with the anomalous Doppler effect [56].

For $V_\perp \neq 0$, the term $V_\perp^2(s^2 + k^2)$ in (4) describes two opposing bunching mechanisms. The azimuthal bunching, represented by k^2, is the dominant amplification mechanism in the fast-wave cyclotron resonance interaction in uniform unloaded waveguides (where $|s| < k$). The axial bunching (Weibel) effect, represented by s^2, is the dominant amplification mechanism in the dielectric-loaded slow-wave ($|s| > k$) cyclotron interaction [31]–[38].

Fig. 3 shows the Lorentz force components which generate the azimuthal and the axial bunching effects, where $\boldsymbol{E}_\perp$ and $\boldsymbol{B}_\perp$ denote the transverse electric and magnetic field components of a TEM plane wave in free-space. The azimuthal bunching stems from the stationary $\boldsymbol{V}_\perp \cdot \boldsymbol{E}_\perp$ product near the cyclotron resonance. The corresponding transverse force $\boldsymbol{F}_\perp$ modulates the electron energy ($\dot{\gamma} = -(e/mc^2)\boldsymbol{V}_\perp \cdot \boldsymbol{E}_\perp$) and slightly varies the cyclotron frequency (2) for electrons in different phases. This relativistic effect occurs also in

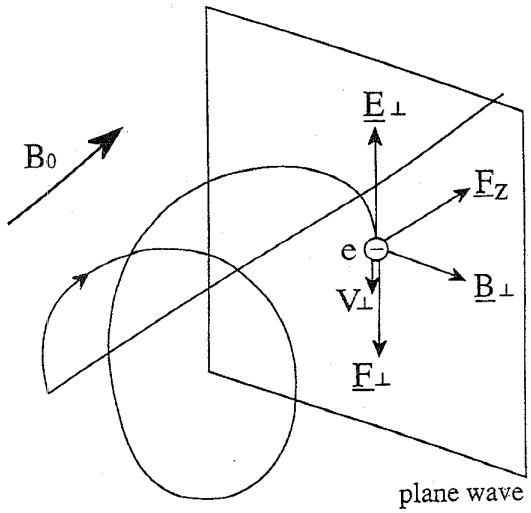

Fig. 3. The azimuthal and axial force components of the TEM–CRM interaction.

low-energy CRM's (as in our 5 keV experiment). The axial-bunching Weibel effect stems from the $\boldsymbol{F}_z = -e\boldsymbol{V}_\perp \times \boldsymbol{B}_\perp$ axial force component as in the ubitron–FEL (free electron laser) interaction.

In a free-space TEM mode, $V_{ph} = c$, the approximate tuning relation (1) for forward or backward waves ($k_z = \pm k$, respectively) is

$$\omega = \frac{n\omega_c}{1 \mp V_z/c}. \tag{5}$$

The term $s^2 + k^2$ in (4) is small in this case since $s \cong \pm jk$. Hence, the azimuthal and the axial bunching effects are almost equal and opposite and they tend to cancel one another. An analysis of (3) and (4) shows that the EM wave energy is absorbed in the cyclotron interaction by the e beam, unless the initial transverse velocity of the electrons is extremely large [15], [46]. The condition for a forward wave amplification in this case is

$$V_\perp > \sqrt{V_z(c - V_z)}. \tag{6}$$

This result differs by a factor of two from a similar known condition [15] due to the inclusion of nonresonant terms in the small-signal analysis here (see [15, Sec. 6]). In this condition (6), the power growth rate of the amplified quasi-TEM wave results from (3) and (4) as

$$P_{\text{out}} \cong \frac{1}{4} P_{\text{in}} \exp\left[\frac{1}{2c}\omega_{pr}\tau_0\sqrt{V_\perp^2 - V_z(c - V_z)}\right] \tag{7}$$

where P_{in} and P_{out} are the input and output EM wave power, respectively, and $\tau_0 = L/V_z$ is the electron transit time in the interaction region.

For a large pitch ratio ($V_\perp/V_z \gg 1$), the empty-waveguide TEM mode is modified in the bound interaction region to a quasi-TEM wave ($|s| \cong k$, according to the dispersion relation (3) poles). The dielectric properties of the rotating electron beam violate the balance of the axial and the azimuthal bunching effects, and a net gain is feasible.

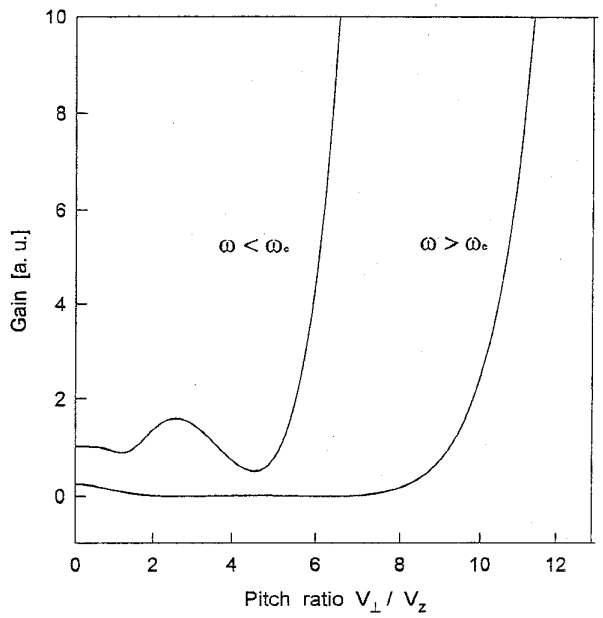

Fig. 4. Power growth of the TEM–cyclotron interaction with the forward and backward wave versus the pitch ratio $V_\perp/V_z$.

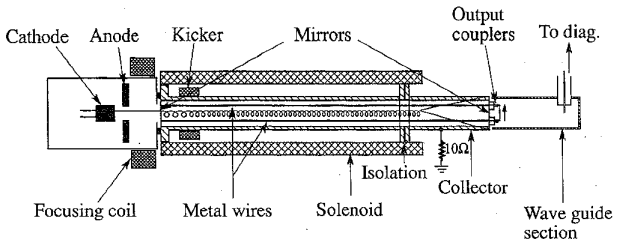

Fig. 5. The TEM–CRM oscillator experimental device.

For a nonrelativistic electron beam, the amplification condition in (6) dictates a very small axial velocity of the electron beam. Hence, the Doppler shift in (5) is relatively small, and $\omega \sim \omega_c$. In addition, the electron transit time in the interaction region, τ_0, becomes larger for a given interaction length. For instance, a 5-keV electron beam ($\beta \sim 0.14$) should propagate with $\beta_z < 0.02$ ($\tau_0 > 0.15$ μs per meter) in order to satisfy the amplification condition of (6), where $\beta_z = V_z/c$. The relatively long transit time of the electrons in the interaction region in this scheme intensifies the effect of the electron density [according to $\omega_{pr}\tau_0$ in (7)], and consequently increases the amplification.

Fig. 4 shows the power growth of forward ($\omega > \omega_c$) and backward ($\omega < \omega_c$) waves computed numerically by (3) and (4) for the experimental parameters given in Table I. The power growth rates are presented in Fig. 4 with respect to the pitch ratio $V_\perp/V_z$. The results show that the cyclotron interaction with a backward wave produces a significant power growth for a pitch ratio of $V_\perp/V_z > 6$, whereas the interaction with a forward wave requires a pitch ratio of $V_\perp/V_z > 10$ for amplification. The CRM synchronism with the backward wave may also excite an absolute instability [29]. Otherwise, oscillations may build up by the feedback mechanism provided by the cavity mirrors and the CRM amplifying medium.

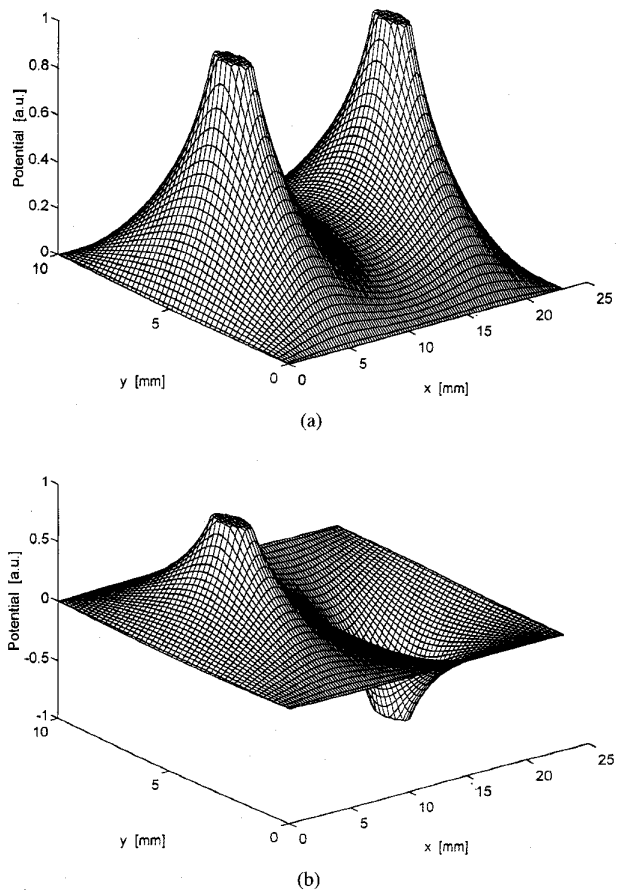

Fig. 6. The even (a) and odd (b) TEM modes of the parallel-line waveguide.

TABLE I
TEM–CRM EXPERIMENTAL PARAMETERS

electron beam		
energy	<5	[keV]
current	<1	[A]
pulsewidth	~1	[ms]
Magnetic field		
solenoid	1–3	[kG]
kicker	~20	[kA turns]
TEM waveguide		
rectangular tube	0.9 × 0.4	[inch^2]
length	75	[cm]
parallel wires:		
wire diameter	1.9	[mm]
distance between centers	11	[mm]
Frequency range		
first harmonic	3.5–6	[GHz]
second harmonic	~7	[GHz]

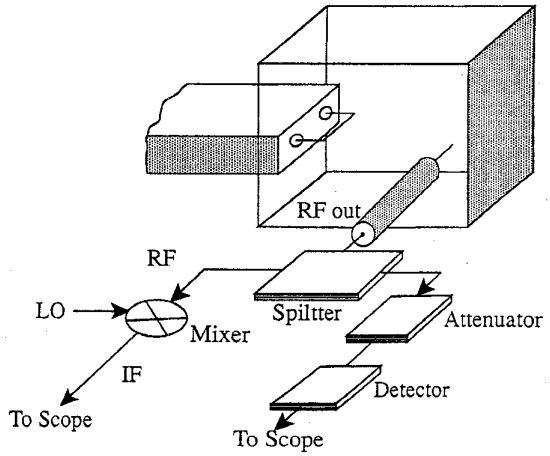

Fig. 7. The microwave diagnostic setup. The radiation is coupled out and split to a frequency heterodyne arm and to a power detector arm.

III. EXPERIMENTAL SETUP

A general view of the table-top experimental CRM device is shown in Fig. 5. The apparatus is based on the setup of the periodic-waveguide CRM experiment at Tel Aviv University [42]. This setup is used for various CRM experiments, and for a low-voltage free-electron maser experiment [57]. The oscillator tube consists of a planar-diode electron gun, a nondispersive parallel-line waveguide (shown in Fig. 1), a solenoid, and a kicker electromagnet which imparts transverse velocity to the electrons. A low-energy electron beam (<5 keV) is injected into the waveguide and interacts with the TEM wave. The uniform solenoidal magnetic field maintains the electron cyclotron motion along its axis. The electron beam is dumped at the exit of the interaction region onto a collector which is also used to measure the electron current.

Three synchronized pulsers generate the solenoid, the e-gun, and the kicker pulses, as described in [42]. The e-gun high-voltage pulser (5 kV, 1 A, 1 ms) [58] and the high-current kicker pulser are triggered at the peak of the 25-ms width solenoid pulse.

The TEM-mode waveguide shown in Fig. 1 consists of two metal wires stretched along a standard WR90 rectangular waveguide. The wires are supported by two small ceramic (Macor) holders at the center of the waveguide. The dimensions of the waveguide are given in Table I.

The computed transverse profiles of the even and odd TEM modes of the parallel-line waveguide, shown in Fig. 6(a) and (b), respectively, are derived from the Laplace equation with the appropriate boundary conditions. The impedance of the parallel-line waveguide in both odd and even modes is measured and calculated to be ~0.2 kΩ.

The waveguide is terminated in the CRM oscillator by two partial mirrors at both ends. The mirror near the electron gun has a hole at the center for the electron beam entrance. The mirror at the collector has an SMA (50 Ω) RF connector attached to each wire. These terminations form a cavity with a low quality factor ($Q < 200$). Cold measurements (in the absence of the electron beam) of the parallel-line waveguide were done on an HP8575A network analyzer [42]. The transmission and reflection measurements of the 75-cm long cavity show resonance frequencies separated by ~200 MHz. The axial modes are almost equally spaced in the frequency domain except for a small deviation related to the reactive loads at the ends of the waveguide.

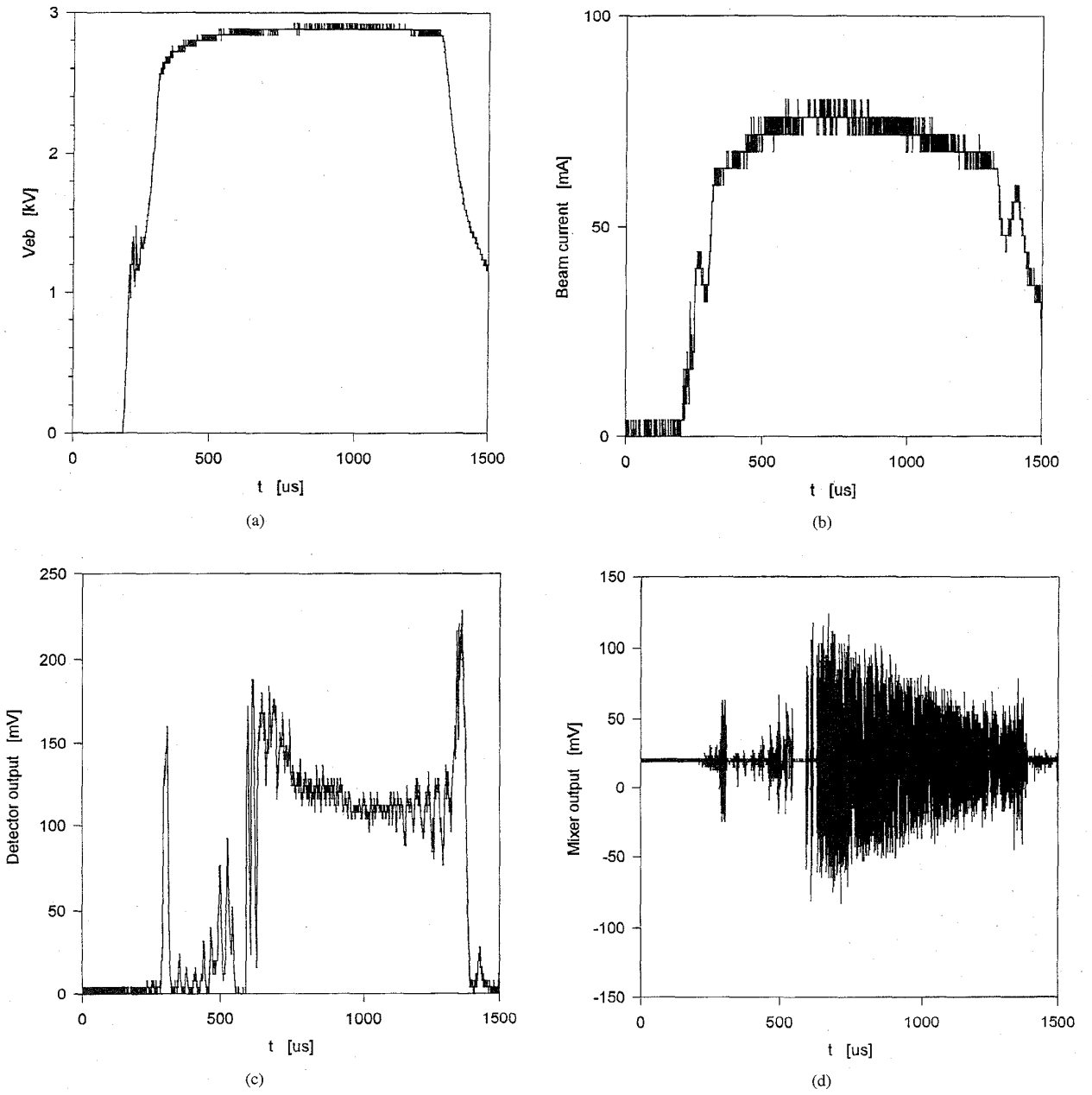

Fig. 8. Typical experimental results of the TEM–CRM oscillator. (a) The electron gun voltage. (b) The electron beam current measured in the collector. (c) The microwave detected output power. (d) The heterodyne mixer output.

The low-energy electron beam is generated by a simple planar diode electron gun, which consists of a dispenser thermionic cathode (Spectra-Mat, STD200) and a planar anode. The electron beam diameter is 4 mm and its filling factor for the odd TEM-mode in Fig. 6(b) is found to be $F_f = 0.026$. The electron optics shown schematically in Fig. 5 consists of a kicker coil which spins up the electron beam. A 1–2 kG solenoidal field is induced along the beam axis. The axial solenoid field drops at the ends (hence, the coherence of the cyclotron frequency is slightly degraded). The waveguide terminated by a collector section is connected to ground through a 10-Ω resistor. The voltage drop on this resistor during the pulse yields the electron current. The effect of the kicker coil as a means to spin up the electrons is studied by a trajectory simulation. The simulation shows that a portion of the electron beam is completely stopped in the z direction. The entire kinetic energy of these electrons is transferred from the initial V_z velocity component to $V_\perp$ by the kicker action (thus their pitch ratio is $V_\perp/V_z \rightarrow \infty$). Another portion of the electron beam satisfies the CRM amplification condition (6). The rest of the electrons have a large spread in V_z.

The RF power generated in the cyclotron oscillator is detected by the apparatus shown in Fig. 7. The output signal is sampled by a small dipole antenna leading into a WR187

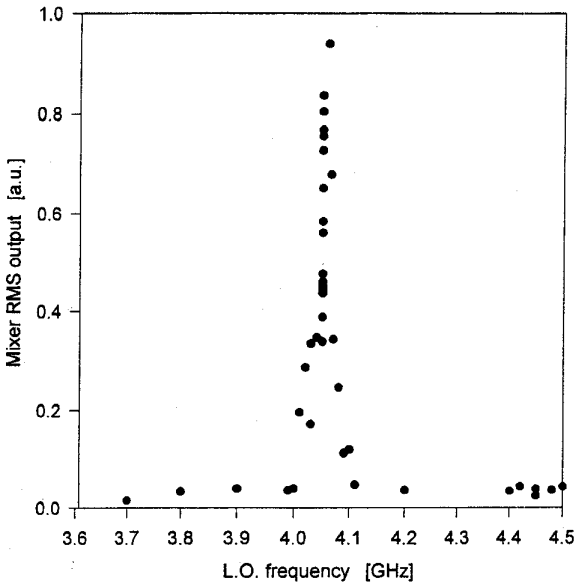

Fig. 9. The linewidth of the CRM oscillator. The dots represent the mixer IF output (rms) for different LO frequencies in various shots. The axial magnetic field is $B_0 = 1.52$ kG.

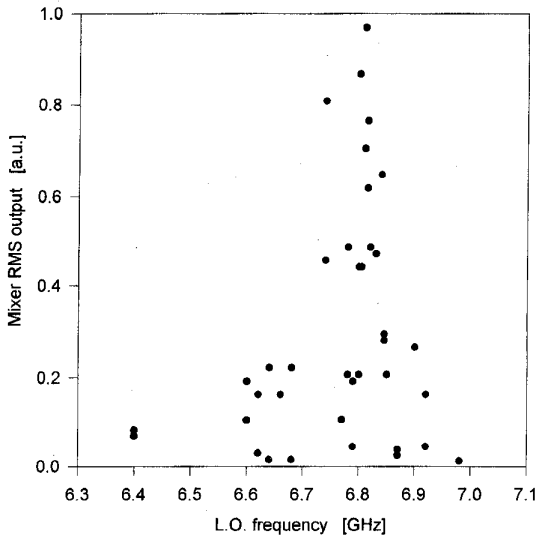

Fig. 10. The CRM emission at second-harmonic frequencies. The dots represent the mixer IF output (rms) for different LO frequencies in various shots. The axial magnetic field is $B_0 \cong 1.35$ kG.

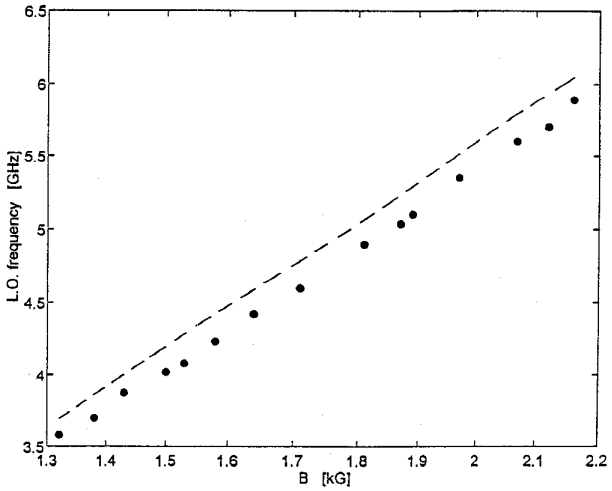

Fig. 11. The center frequency of the CRM output at the fundamental harmonic versus the axial magnetic field. The dashed line shows the corresponding cyclotron frequency.

waveguide section which acts as a high-pass filter (its cutoff frequency is 3.15 GHz). The signal is received by a coaxial probe and is split into two arms. In the power measurement arm the signal is attenuated and detected by an HP8474C power detector. In the heterodyne measurement arm the signal is mixed with a fixed local-oscillator (LO) signal from an external RF oscillator. The mixer output is filtered by the internal 20-MHz low-pass filter of a Tektronix TDS 540 digital oscilloscope. This heterodyne measurement shows the spectral contents of the CRM oscillator output shifted by the LO frequency. Typical output signal measurements are presented in the next section.

IV. Experimental Results

Typical results of the CRM oscillator experiment are shown in Fig. 8(a), (b), (c), and (d). Fig. 8(a) and (b) shows the electron gun voltage variation during the pulse and the corresponding electron beam current measured in the collector section, respectively. Fig. 8(c) and (d) shows the microwave power detector output and the corresponding microwave heterodyne detection output, respectively. The output signal of the mixer shown in Fig. 8(d) is observed with an LO frequency of $f_{\mathrm{LO}} \cong 4.4$ GHz and a solenoid field of $B_0 \cong 1.6$ kG. The corresponding cyclotron frequency ($f_c \cong 4.7$ GHz) is slightly higher than the radiation frequency.

The spectral content of the CRM oscillator emission is measured by varying the LO frequency from pulse to pulse with the same axial magnetic field. The dots in Fig. 9 represent the rms values of the mixer IF-output in different LO frequencies. The axial magnetic field in these runs is $B_0 \cong 1.5$ kG, which corresponds to $f_c \cong 4.2$ GHz. According to the tuning relation of (5), $f = nf_c/(1 \pm \beta_z)$, the deviation of the center frequency in Fig. 9, $f \cong 4.05$ GHz, from the cyclotron frequency corresponds to $\beta_z \cong 0.04$, and to an interaction with a backward wave. Consequently, the CRM operates with a pitch ratio $V_\perp/V_z \geq 2.5$. The total electron velocity in this experiment is $|V| \cong 0.11c$, and most of it is imparted to the transverse cyclotron motion in agreement with theory (Fig. 4). The CRM linewidth (full width at half maximum) is measured in Fig. 9 to be $\Delta f \cong 0.1$ GHz. The axial velocity spread which may cause this line widening is $\Delta\beta_z \cong 0.02$ [assuming that $\Delta\beta_z \sim (1 - \overline{\beta}_z)^2 \Delta\omega/\omega_c$ as results from (5)].

Radiation bursts at second-harmonic frequencies are observed in different axial magnetic fields. Fig. 10 shows the second-harmonic spectral content as measured by varying the LO frequency from pulse to pulse, as in Fig. 9. The dots in Fig. 10 represent the rms values of the mixer IF-output in different LO frequencies in the second harmonic range. The axial magnetic field in these runs is $B_0 \cong 1.35$ kG, which

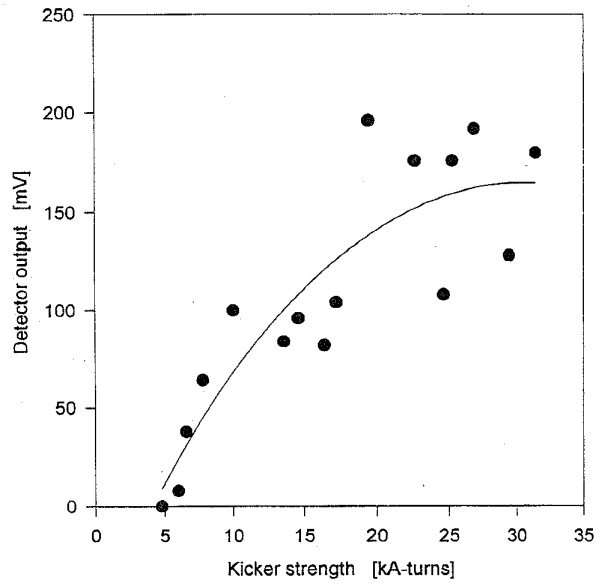

Fig. 12. The effect of the kicker strength on the CRM radiation emission.

corresponds to $f_c \cong 3.65$ GHz. In these runs the emission in the second harmonic is stronger than in the fundamental harmonic, probably because it is better tuned to the cavity mode. The measured RF center frequency, ~6.8 GHz, is slightly lower than the second-harmonic cyclotron frequency, 7.3 GHz, and consequently, the interaction occurs with a backward wave, as the fundamental harmonic interaction.

The CRM oscillator frequency is tuned by varying the solenoid field. CRM tunability is demonstrated over almost one octave in this experiment, at the frequency range 3.5–6.0 GHz (in the first harmonic). Lower frequencies are measured as well without the high-pass filter at the exit of the cavity. The dots in Fig. 11 represent the LO frequencies in which the maximum IF outputs (rms) are obtained at each value of the axial magnetic field. The RF frequency line in Fig. 11 is lower than the cyclotron frequency line (shown in a dashed line) by a factor of $\omega/\omega_c \sim 0.96$, in agreement with the theory discussed above.

The effect of the kicker field is observed by varying the magnetic strength produced by the kicker coil shown in Fig. 5. The relation between the radiation output and the kicker strength is shown in Fig. 12. No radiation is observed below a threshold in the kicker field of 5 kA-turns. The optimal kicker strength in this experiment is ~20 kA-turns. The typical output RF power extracted from the cavity in this case is ~10 W, which corresponds to an extraction efficiency of ~2%. In larger kicker fields the focusing of the electron beam is deteriorated.

V. Conclusions

The cyclotron maser oscillator experiment presented in this paper shows a cyclotron interaction between a low-energy electron beam orbiting in an axial magnetic field and a TEM wave in a nondispersive waveguide. The coupling occurs only with a considerable kicker field. The kicker induces a large transverse electron velocity component, as required by the CRM linear model. A wide tunability of the CRM interaction in a nondispersive waveguide is demonstrated in this experiment. A considerable emission is observed also at second-harmonic frequencies.

A further study is needed to investigate the effects of the electron velocity spread. Novel kicker mechanisms and higher harmonic interactions should be examined in order to improve the performance of the CRM device. Our recent experiment shows, however, the feasibility of a nonrelativistic CRM device in a nondispersive metallic waveguide.

References

[1] J. L. Hirshfield and V. L. Granatstein, "The electron cyclotron maser—A historical survey," *IEEE Trans. Microwave Theory Tech.*, vol. MTT-25, pp. 522–527, 1977; and references therein.

[2] R. Q. Twiss, "Radiation transfer and the possibility of negative absorption in radio astronomy," *Aust. J. Phys.*, vol. 11, pp. 564–579, 1958.

[3] J. Schneider, "Stimulated emission of radiation by relativistic electrons in a magnetic field," *Phys. Rev. Lett.*, vol. 2, pp. 504–505, 1959.

[4] A. V. Gaponov, "Interaction between electron fluxes and electromagnetic waves in waveguides," *Izv. VUZ Radiofizika*, vol. 2, pp. 450–462, 1959.

[5] K. K. Chow and R. H. Pantell, "The cyclotron resonance backward wave oscillator," *Proc. IEEE*, vol. 48, pp. 1865–1870, 1960.

[6] G. Bekefi, J. L. Hirshfield, and S. C. Brown, "Cyclotron emission from plasmas with non-Maxwellian distributions," *Phys. Rev.*, vol. 122, pp. 1037–1042, 1961.

[7] I. B. Bott, "Tunable source of millimeter and sub-millimeter electromagnetic radiation," *Proc. IEEE*, vol. 52, pp. 330–331, 1964.

[8] J. L. Hirshfield and J. M. Wachtel, "Electron cyclotron maser," *Phys. Rev. Lett.*, vol. 12, pp. 533–536, 1964.

[9] J. L. Hirshfield, I. B. Bernstein, and J. M. Wachtel, "Cyclotron resonance interaction of microwaves with energetic electrons," *IEEE J. Quantum Electron.*, vol. QE-1, pp. 237–245, 1965.

[10] A. V. Gaponov, M. I. Petelin, and V. K. Yulpatov, "The induced radiation of excited classical oscillators and its use in high-frequency electronics," *Izv. VUZ Radiofiz.* vol. 10, pp. 1414–1454, 1967; *Radiophys. Quantum Electron.*, vol. 10, pp. 794–814, 1967.

[11] V. L. Granatstein, M. Herndon, R. K. Parker, and P. Sprangle, "Coherent synchrotron radiation from an intense relativistic electron beam," *IEEE J. Quantum Electron.*, vol. QE-10, pp. 651–654, 1974.

[12] N. I. Zaytsev, T. V. Pankratova, M. I. Petelin, and V. A. Flyagin, "Millimeter- and submillimeter-wave gyrotrons," *Radio Eng. Electron. Phys.*, vol. 19, pp. 103–107, 1974.

[13] D. V. Kisel, G. S. Korablev, V. G. Pavel'yev, M. I. Petelin, and Sh. Ye. Tsimring, "An experimental study of a gyrotron operating at the second harmonic of the cyclotron frequency, with optimized distribution of the high-frequency field," *Radio Eng. Electron. Phys.*, vol. 19, pp. 95–100, 1974.

[14] V. A. Flyagin, A. V. Gaponov, M. I. Petelin, and V. K. Yulpatov, "The gyrotron," *IEEE Trans. Microwave Theory Tech.*, vol. MTT-25, pp. 514–521, 1977.

[15] V. L. Bratman, N. S. Ginzburg, G. S. Nusinovich, M. I. Petelin, and P. S. Strelkov, "Relativistic gyrotrons and cyclotron autoresonance masers," *Int. J. Electron.*, vol. 51, pp. 541–567, 1981.

[16] S. Y. Park, R. H. Kyser, C. M. Armstrong, R. K. Parker, and V. L. Granatstein, "Experimental study of a Ka-band gyrotron backward-wave oscillator," *IEEE Trans. Plasma Sci.*, vol. 18, pp. 321–325, 1990.

[17] T. Idehara, T. Tatsukawa, S. Matsumoto, K. Kunieda, K. Hemmi, and T. Kanemaki, "Development of high-frequency cyclotron harmonic gyrotron oscillator," *Phys. Lett. A*, vol. 132, pp. 344–346, 1988.

[18] S. Spira-Hakkarainen, K. E. Kreischer, and R. J. Temkin, "Submillimeter-wave harmonic gyrotron experiment," *IEEE Trans. Plasma Sci.*, vol. 18, pp. 334–342, 1990.

[19] C. S. Kou, D. B. McDermott, N. C. Luhmann, Jr., and K. R. Chu, "Prebunched high-harmonic gyrotron," *IEEE Trans. Plasma Sci.*, vol. 18, pp. 343–349, 1990.

[20] G. F. Brand, P. W. Fekete, K. Hong, K. J. Moore, and T. Idehara, "Operation of a tunable gyrotron at the second harmonic of the electron cyclotron frequency," *Int. J. Electron.*, vol. 68, pp. 1099–1111, 1990.

[21] N. A. Nikolov, I. P. Spasovsky, K. G. Kostov, J. N. Velichkov, V. A. Spasov, and I. G. Yovchev, "Cyclotron autoresonance maser in the millimeter region," *J. Appl. Phys.*, vol. 67, no. 12, pp. 7620–7622, 1990.
[22] A. C. DiRienzo, G. Bekefi, C. Chen, and J. S. Wurtele, "Experimental and theoretical studies of a 35 GHz cyclotron autoresonance maser amplifier," *Phys. Fluids*, vol. B3, pp. 1755–1765, 1991.
[23] P. B. Park, "A direct solution for the efficiency and gain of a CARM oscillator," *IEEE Trans. Plasma Sci.*, vol. 18, pp. 223–227, 1990.
[24] J. M. Baird, "Gyrotron theory," in *High Power Microwaves*, V. L. Granatstein and I. Alexeff, Eds. Boston: Artech House, 1987; and references therein.
[25] R. G. Kleva, B. Levush, and P. Sprangle, "Radiation focusing in the cyclotron autoresonance maser," *Phys. Fluids*, vol. 31, pp. 3171–3173, 1988.
[26] C. Chen and J. S. Wurtele, "Efficiency enhancement in cyclotron autoresonance maser amplifiers by magnetic field tapering," *Phys. Rev. A*, vol. 40, pp. 489–492, 1989.
[27] A. W. Fliflet and W. M. Manheimer, "Nonlinear theory of phase-locking gyrotron oscillators driven by an external signal," *Phys. Rev. A*, vol. 39, pp. 3432–3443, 1989.
[28] R. C. Davidson and P. H. Yoon, "Stabilization of the cyclotron autoresonance maser instability by axial momentum spread," *Phys. Rev. A*, vol. 39, pp. 2534–2538, 1989.
[29] J. C. Davies, "Conditions for absolute instability in the cyclotron resonance maser," *Phys. Fluids B*, vol. 1, pp. 663–669, 1989.
[30] A. Fruchtman and L. Friedland, "Theory of a nonwiggler collective free electron laser in uniform magnetic field," *IEEE J. Quantum Electron.*, vol. QE-19, pp. 327–333, 1983.
[31] K. R. Chu, A. K. Ganguly, V. L. Granatstein, J. L. Hirshfield, S. Y. Park, and J. M. Baird, "Theory of a slow wave cyclotron amplifier," *Int. J. Electron.*, vol. 51, pp. 493–502, 1981.
[32] H. Guo, L. Chen, H. Keren, and J. L. Hirshfield, "Measurements of gain for slow cyclotron wave on an annular electron beam," *Phys. Rev. Lett.*, vol. 49, pp. 730–733, 1982.
[33] H. S. Uhm and J. Y. Choe, "Gyrotron amplifier in a helix loaded waveguide," *Phys. Fluids*, vol. 26, pp. 3418–3425, 1983.
[34] N. T. Cherpak and T. A. Smirnova, "Gyromagnetic perturbation of the delay structure in a mm-band maser," *Sov. J. Commun. Technol. Electron.*, vol. 30, pp. 74–81, 1985.
[35] D. B. McDermott, H. B. Cao, and N. C. Luhmann, "Cherenkov cyclotron autoresonance maser," *Int. J. Electron.*, vol. 65, pp. 477–482, 1988.
[36] T. H. Kho and A. T. Lin, "Slow wave electron cyclotron maser," *Phys. Rev. A*, vol. 38, pp. 2883–2888, 1988.
[37] A. K. Ganguly and S. Ahn, "Nonlinear theory for the slow wave cyclotron interaction," *Phys. Rev. A*, vol. 42, pp. 3544–3554, 1990.
[38] K. C. Leou, D. B. McDermott, and N. C. Luhmann, Jr., "Dielectric-loaded wideband gyro-TWT," *IEEE Trans. Plasma Sci.*, vol. 20, pp. 188–196, 1992.
[39] K. R. Chu and J. L. Hirshfield, "Comparative study of the axial and azimuthal bunching mechanisms in electromagnetic cyclotron instabilities," *Phys. Fluids*, vol. 21, pp. 461–466, 1978.
[40] E. Jerby and G. Bekefi, "Cyclotron maser experiments in a periodic waveguide," *Phys. Rev. E*, vol. 48, pp. 4637–4641, 1993.
[41] E. Jerby, G. Bekefi, and A. Shahadi, "Observation of chirping in a traveling-wave cyclotron maser experiment," *Nucl. Instrum. Methods*, vol. A341, pp. 115–118, 1994.
[42] E. Jerby, A. Shahadi, V. Grinberg, V. Dikhtiar, M. Sheinin, E. Agmon, H. Golombek, V. Trebich, M. Bensal, and G. Bekefi, "Cyclotron maser oscillator experiments in a periodically loaded waveguide," *IEEE J. Quantum Electron.*, vol. 31, pp. 970–979, 1995.
[43] E. Jerby, "Linear analysis of periodic waveguide cyclotron maser," *Phys. Rev. E*, vol. 49, pp. 4487–4496, 1994.
[44] S. K. Ride and W. B. Colson, "A free electron laser in a uniform magnetic field," *Appl. Phys.*, vol. 20, pp. 41–50, 1979.
[45] A. Fruchtman, "Wiggler-free free electron waveguide laser in a uniform axial magnetic field: Single particle treatment," *J. Appl. Phys.*, vol. 54, pp. 4289–4294, 1983.
[46] F. A. Korolev and A. F. Kurin, "Cyclotron-resonance maser with a Fabry–Perot cavity," *Radio Eng. Electron. Phys.*, vol. 15, pp. 1868–1873, 1970.
[47] E. C. Morse and R. V. Pyle, "Operation of a quasioptical electron cyclotron maser," *J. Vac. Sci. Technol. A.*, vol. 3, pp. 1239–1240, 1985.
[48] N. A. Ebrahim, Z. Liang, and J. L. Hirshfield, "Bernstein-mode quasioptical maser experiment," *Phys. Rev. Lett.*, vol. 49, pp. 1556–1560, 1982.
[49] A. F. Kurin, G. A. Kurina, and V. V. Novikov, "Nonlinear theory of a cyclotron-resonance maser with a Fabry–Perot resonator," *Radiophys. Quantum Electron.*, vol. 19, pp. 742–747, 1976.
[50] P. Sprangle, J. L. Vomvoridis, and W. M. Manheimer, "A classical electron cyclotron quasioptical maser," *Appl. Phys. Lett.*, vol. 38, pp. 310–313, 1981.
[51] A. Bondeson, B. Levush, W. M. Manheimer, and E. Ott, "Multimode theory and simulation of quasioptical gyrotrons and gyroklystrons," *Int. J. Electron.*, vol. 53, pp. 547–553, 1982.
[52] T. F. Dikun, S. V. Kolosov, A. A. Kurayev, and B. M. Paramonov, "Cascade interaction of a relativistic electron stream with T_{00n} fields of open resonators in the presence of uniform electric and magnetic fields," *Sov. J. Commun. Technol. Electron.*, vol. 31, no. 12, pp. 158–165, 1986.
[53] C. M. Tang, S. Riyopoulos, P. Sprangle, and B. Levush, "Operation of the induced resonance electron cyclotron maser at higher harmonics," *Nucl. Instrum. Methods Phys. Res.*, vol. A252, pp. 192–197, 1987.
[54] A. W. Fliflet, T. A. Hargreaves, W. M. Manheimer, R. P. Fischer, and M. L. Barsanti, "Initial operation of a higher-power quasioptical gyrotron," *IEEE Trans. Plasma Sci.*, vol. 18, pp. 306–312, 1990.
[55] A. Shahadi, E. Jerby, M. Korol, R. Drori, M. Sheinin, V. Dikhtiar, V. Grinberg, I. Ruvinsky, M. Bensal, T. Harhel, Y. Baron, A. Fruchtman, V. L. Granatstein, and G. Bekefi, "Cyclotron resonance maser experiment in a nondispersive waveguide," in *Proc. 16th Int. FEL Conf.*, Stanford, CA, Aug. 1994, in *Nucl. Instrum. Methods Phys. Res.*, vol. A358, pp. 143–146, 1995.
[56] M. V. Kuzelev and A. A. Rukhadze, "Stimulated radiation from high-current relativistic electron beams," *Sov. Phys. Usp.*, vol. 30, pp. 507–524, 1987.
[57] R. Drori, E. Jerby, and A. Shahadi, "Free-electron maser oscillator experiment in the UHF regime," *Nucl. Instrum. Methods*, vol. A358, pp. 151–154, 1995.
[58] V. Grinberg, E. Jerby, and A. Shahadi, "Low-cost electron-gun pulser for table-top maser experiments," *Nucl. Instrum. Methods*, vol. A358, pp. 327–330, 1995.

Eli Jerby received the B.Sc. and M.Sc. degrees in 1980, and the Ph.D. degree in 1989, all from Tel Aviv University, Israel.

In 1989–1990, he was a postdoctoral Fulbright and Rothschild Fellow at the Massachusetts Institute of Technology, Cambridge, under the supervision of Prof. G. Bekefi. He returned to Tel Aviv University in 1991, and established a high-power microwave generation laboratory. He conducts and supervises studies on new schemes of low-voltage cyclotron-resonance and free-electron masers.

Avi Shahadi received the B.Sc. and M.Sc. degrees (magna cum laude) in electrical engineering from Tel Aviv University, Israel, in 1993 and 1996, respectively. Currently, he is a Ph.D. student in the High-Power Microwave Laboratory at Tel Aviv University. His dissertation work deals with a novel infrared radiation source based on a cyclotron-resonance maser.

Rami Drori received the B.Sc. degree in physics from Bar-Ilan University, Israel, in 1988, and the M.Sc. degree in electrical engineering from Tel Aviv University, Israel, in 1994 (both magna cum laude). Currently, he is a Ph.D. student in the High-Power Microwave Laboratory. His major research subject is a low-voltage (<1 kV) free-electron maser operating in the VHF range.

Michael Korol received the M.S. degree in physics from Ural State University, U.S.S.R., in 1987. He emigrated to Israel in 1991. Currrently, he is a Ph.D. student in the High-Power Microwave Laboratory at Tel Aviv University, Israel. His research work concentrates in the theory of novel cyclotron-resonance maser schemes.

Moshe Einat received the B.Sc. degree in electrical engineering in 1988 from Tel Aviv University, Israel, from where he is currently pursuing the M.Sc. degree. His thesis work includes dielectric-loaded cyclotron and free-electron maser experiments.

Marat Sheinin received the M.Sc. degree in radio technology from the Institute of Minsk, U.S.S.R., in 1962.

He worked in Russia as a Microwave Engineer until he emigrated to Israel in 1990. He joined the High-Power Microwave Laboratory at Tel Aviv University, Israel, in 1992 in the position of Visiting Research Engineer.

Vladimir Dikhtiar received the M.S. degree in radiophysics from the National University of Sarato, Russia, in 1970, and the Ph.D. degree in electrical engineering from the Moscow Institute of Radio-Engineering and Electronics of the U.S.S.R. Academy of Sciences in 1975.

In 1975, he joined the Moscow Institute of Radio-Engineering and Electronics as a Research Associate. He emigrated to Israel in 1991. Currently, he is a Research Associate at the High-Power Microwave Laboratory, Tel Aviv University, Israel. His major research interest is a scattering analysis of active and passive microwave devices.

Vladimir Grinberg received the Cand.Sc. degree in 1974 from the Polytechnic Institute of Tomsk, Russia.

During 1992–1996, he was a Visiting Scientist at the High-Power Microwave Laboratory, Tel Aviv University, Israel. He is specialized in electrical machines, electromotors with built-in brakes, transient processer theory, and electromagnet systems with magnetic-field forcing.

Moshe Bensal was a Microwave Technician at Elisra Ltd. between 1978 and 1987, when he joined Tel Aviv University, Israel. He is the Chief Technician of the High-Power Microwave Laboratory at Tel Aviv University.

Tal Harhel received the Technical Engineer degree from Tel Aviv Technical College, Israel, in 1995. His thesis project conducted at the High-Power Microwave Laboratory included the development of CRM subsystems.

Yitzchak Baron is currently pursuing the Technical Engineer degree from Tel Aviv Technical College, Israel. His thesis project conducted at the High-Power Microwave Laboratory included the development of CRM subsystems.

Amnon Fruchtman (M'95) received the B.Sc. degree in 1973 from Tel Aviv University, and the M.Sc. and Ph.D. degrees in 1978 and 1983, respectively, both from the Hebrew University of Jerusalem, Israel.

He worked as a Postdoctoral Fellow during 1983–1986 at the Courant Institute, New York University, and during 1986–1995 was on the faculty of the Weizmann Institute of Science, Rehovot, Israel. He has recently joined the Center for Technological Education, Holon, as an Associate Professor. His research topics include various aspects of plasma physics, such as plasma waves and instabilities, plasma diodes and switches, electric propulsion, and free electron lasers.

Dr. Fruchtman is a member of the American Physical Society.

Victor L. Granatstein (S'59–M'64–SM'86–F'92), for a photograph and biography, see this issue, p. 665.

George Bekefi, for a photograph and biography, see this issue, p. 556.